



A superconducting detector endstation for high-resolution energy-dispersive SR-XRF

S. Friedrich^{a,b,*}, T. Niedermayr^a, O. Drury^a, M.F. Cunningham^a,
M.L. van den Berg^a, J.N. Ullom^a, A. Loshak^a, T. Funk^b, S.P. Cramer^b,
J.D. Batteux^a, E. See^a, M. Frank^a, S.E. Labov^a

^aLawrence Livermore National Laboratory, P.O. Box 808, L-418, Livermore, CA 94551, USA

^bLawrence Berkeley National Laboratory, MS 6-2100, Berkeley, CA 94720, USA

Abstract

We have built a two-stage adiabatic demagnetization refrigerator (ADR) to operate cryogenic high-resolution X-ray detectors in synchrotron-based fluorescence applications. The detector is held at the end of a 40 cm cold finger that extends into a UHV sample chamber. The ADR attains a base temperature below 100 mK with about 20 h hold time below 400 mK, and does not require pumping on the liquid He bath. We will discuss cryostat design and performance. © 2001 Elsevier Science B.V. All rights reserved.

Keywords: Adiabatic demagnetization refrigerators; Superconducting tunnel junctions; X-ray detectors

1. Introduction

Cryogenic X-ray detectors have received wide attention during the last decade because they combine the high energy resolution of grating spectrometers with the broadband efficiency of semiconducting energy-dispersive detectors [1]. Cryogenic detectors for the photon energy range between 0.1 and 6 keV fall into two groups: microcalorimeters, which offer very high energy resolution between 2 and 5 eV FWHM at the expense of low count rate around 500 counts/s [2,3], and superconducting tunnel junctions (STJs),

which offer somewhat poorer resolution between 2 and 13 eV FWHM but can be operated at an order of magnitude higher count rates [4–6].

High energy resolution combined with comparably high count rate capabilities makes STJ detectors attractive for synchrotron-based X-ray fluorescence spectroscopy (SR-XRF). We have developed Nb–Al–AlO_x–Al–Nb STJ detectors and operated them in an adiabatic demagnetization refrigerator (ADR) in SR-XRF applications [6,7]. Our STJ detectors have achieved an energy resolution between 1.7 and 8.9 eV FWHM at 50 eV–1 keV, and they have been successfully operated at count rates above 10,000 counts/s [4,6].

For practical SR-XRF experiments, the STJ detector, typically with an area around

*Corresponding author. Tel.: +1-925-423-1527; fax: +1-925-424-5512.

E-mail address: friedrich1@llnl.gov (S. Friedrich).

$0.1 \times 0.1 \text{ mm}^2$, must be placed close to the sample to acquire data with a reasonable count rate. Also, since the Al vacuum vessel of a typical ADR cryostat cannot be baked out easily, residual gases can freeze out on the STJ detector and on the thin IR blocking windows in front of it. Finally, the necessity to pump on the liquid He bath consumes both time and liquid He. We have therefore designed a new two-stage ADR for SR-XRF where the STJ detector is held at the end of a cold finger that can be inserted into a UHV sample chamber. Here, we discuss the design and performance of this detector system.

2. Cryostat design

Adiabatic demagnetization is a process of magnetic cooling below a liquid He bath temperature through isothermal magnetization and adiabatic demagnetization of a paramagnetic material. Magnetization lowers the entropy of the paramagnet, and the heat of magnetization is carried into a liquid He bath through a closed heat switch. After opening the heat switch, the magnetic field is decreased sufficiently slowly to keep the entropy of the paramagnet constant, thereby lowering its temperature. ADRs are compact, reliable and easy to use.

The ADR cryostat discussed here uses a commercial 30 cm diameter shell with a 7.4 l liquid N_2 and a 9.6 l liquid He tank. The liquid He tank has a cylindrical 10 cm cavity to accommodate the 5 T ADR magnet with the paramagnets and a Vanadium Permendur magnetic shield. To reduce the heat load into the liquid He tank, the the ADR magnet uses high-temperature superconducting BSCCO current leads between the liquid N_2 and liquid He cooled stages.

The cryostat uses two nested stages with two different paramagnets (Fig. 1) [8,3]. The first stage is cooled to a temperature around 1 K by a 143 g single crystal of gadolinium gallium garnet $\text{Gd}_3\text{Ga}_5\text{O}_{12}$ (GGG). This stage supports a second stage which cools to a base temperature below 0.1 K using a home-grown 63 g salt pill of paramagnetic $\text{Fe}(\text{NH}_4)(\text{SO}_4)_2 \times 12\text{H}_2\text{O}$, commonly known as FAA for ferric ammonium alum. This

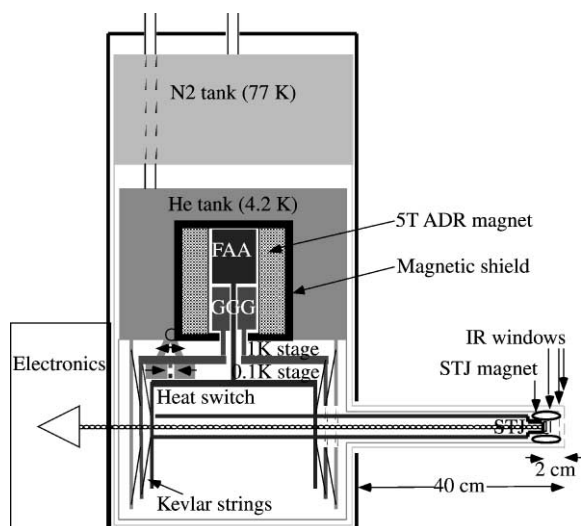


Fig. 1. Schematic cross-section of the two-stage ADR.

two-stage design allows detector operation at a base temperature below 0.1 K with a bath temperature of 4.2 K and thus does not require pumping on the liquid He bath. Since FAA dehydrates at temperatures above 40°C thereby losing its paramagnetic properties, the ADR cannot be baked out easily. We have therefore assembled the ADR in a clean room wearing latex gloves and using only ultrasonically cleaned parts and vented screws to make it as close to UHV compatible as possible.

We operate both paramagnets with a single magnet and a single heat switch. We have designed an electrically controlled mechanical heat switch to avoid air leakage at the O-ring sealed feedthroughs often found in conventional mechanical heat switches (Fig. 2). It uses an over-center-cam locking mechanism activated by 200 ms 1.5 A current pulses through two solenoids that toggle a stainless steel spring between two stable positions. The heat switch provides a force of 1500 N to each of the cold fingers. Its thermal conductance of 65 mW/K at 4.2 K is limited by the thermal conductivity of the OFHC Cu braids between the heat switch and the He bath. After magnetization, the cold stages return to the bath temperature within 30 min. This dominates the time required for a demagnetization cycle.

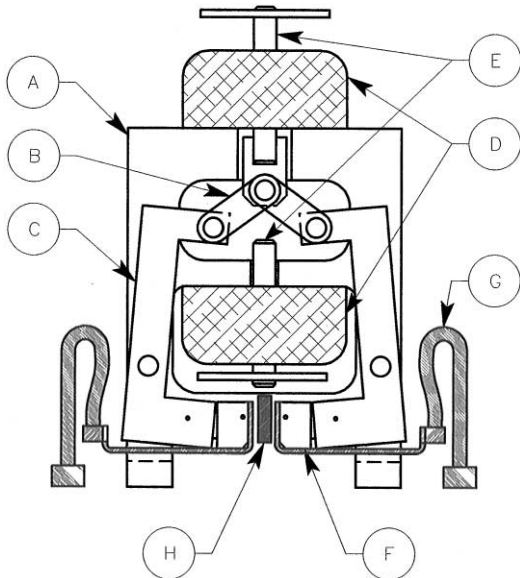


Fig. 2. Schematics of the heat switch: (A) Stainless steel (SS) frame, (B) Movable SS links to, (C) SS springs which rotate about the pivot points (circles), (D) two solenoids (cross-hatched) with plungers (E) for opening (bottom) and closing (top) heat switch, (F) Au-plated OFHC Cu thermal links (shaded), spring-loaded to pivot at the end of the SS springs (C) for good thermal contact between the 0.1 K stage and 1 K stage fingers (H) and the liquid He bath through the annealed OFHC Cu-braids (G).

The STJ detector is mounted at the end of a Au-plated OFHC Cu rod. This rod is surrounded by a liquid He cooled Au-plated OFHC Cu radiation shield, which also holds the STJ detector magnet needed to suppress the dc Josephson current for stable STJ operation. All of this is enclosed with a second radiation shield attached to the liquid N₂ cooled stage. The entire cold finger protrudes 40 cm from the cryostat wall, and its diameter of 45 mm is sufficiently small to fit through standard gate valves. Three 500 Å Al on 2000 Å parylene IR blocking windows on an 85% transmissive Cu grid at the end of the cold finger prevent room temperature radiation from heating the cold stage and causing IR induced excess noise in the detector. Their 5 mm diameter is determined by a trade-off between desired angle of acceptance and tolerable IR photon flux.

3. Results and discussion

Our two-stage ADR has attained a base temperature as low as 60 mK, which allows temperature controlled operation at temperatures down to 80 mK. The cold stage has a hold time of about 20 h below 400 mK, the maximum operating temperature of our STJ detectors. The liquid He hold time is about two days. The total time for a demagnetization cycle is 45 min, yielding a duty cycle for the ADR of more than 95%.

Initial X-ray fluorescence measurements at the Advanced Light Source have achieved an energy resolution between 11 and 25 eV FWHM for photon energies between 277 and 850 eV with $0.1 \times 0.1 \text{ mm}^2$ STJ detectors. This is already more than sufficient to separate even weak transition metal L lines from say a strong oxygen K line, as shown in the emission spectrum of the metalloprotein hydrogenase (Fig. 3). On the other hand, the resolution is less than that of nominally identical STJ detectors mounted in the center of an ADR, rather than at the end of a cold finger

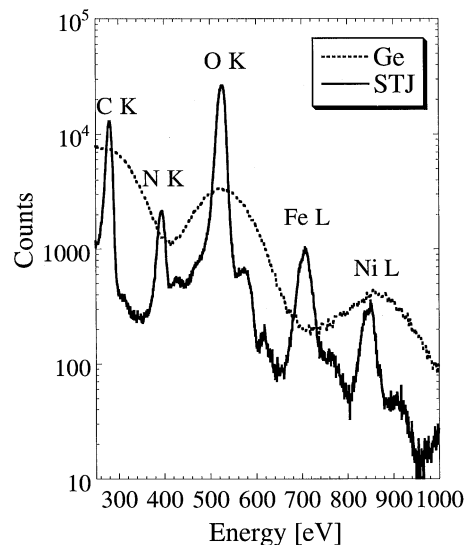


Fig. 3. Soft X-ray emission spectrum of the metalloprotein hydrogenase containing ≈ 480 ppm Ni and ≈ 5800 ppm Fe (solid line). An emission spectrum of this protein taken with a commercial 30-element Ge detector is shown for comparison. The Ni fluorescence is enhanced because of resonant excitation at the Ni L edge (dashed).

within 2.5 cm of a room temperature sample [4,6]. This discrepancy may be due to excess noise caused by IR radiation, or due to insufficient shielding of external magnetic fields. The UHV chamber vacuum was in the low 10^{-9} mbar range, and no signs of gas freeze-out on the IR blocking windows have been observed.

In summary, we have built a two-stage ADR with a 40 cm long cold finger to operate cryogenic STJ detectors in synchrotron-based X-ray fluorescence applications. It allows easy operation of STJ detectors with ≈ 10 –25 eV FWHM resolution at a distance of ≈ 2.5 cm to the sample in a UHV chamber in the low 10^{-9} mbar range. This advance in detector development significantly improves the sensitivity in high-resolution soft X-ray spectroscopy of dilute samples.

Acknowledgements

This work was performed under the auspices of the US Department of Energy by University of California Lawrence Livermore National Labora-

tory under Contract No. W-7405-Eng-48. Funding was provided by the NASA SADD Grant NAG 5-4137, the NASA High Energy Astrophysics SR&T agreement W19.121, the NASA Constellation X program under S-10256G, the NIH Grant GM 44380, the DOE OBER, and the Radiometry Laboratory of the PTB, Berlin. We particularly thank R. Fliegauf, M. Veldkamp and B. Beckhoff for their efforts and feedback.

References

- [1] Proceedings of the Eighth International Workshop on Low Temperature Detectors (LTD-8), Nucl. Instr. and Meth. A 444 (2000).
- [2] K.D. Irwin et al., Nucl. Instr. and Meth. A 444 (2000) 184.
- [3] D.A. Wollman et al., J. Microsc. 188 (1997) 196.
- [4] S. Friedrich et al., IEEE Trans. Appl. Supercond. 9 (1999) 3330.
- [5] G. Angloher et al., Nucl. Instr. and Meth. A 444 (2000) 214.
- [6] M. Frank et al., Rev. Sci. Instrum. 69 (1998) 25.
- [7] S. Friedrich et al., J. El. Spectrosc. Relat. Phenom. 101 (1999) 891.
- [8] C. Hagmann, P.L. Richards, Cryogenics 34 (1994) 221.